The Ameliorating Effect of Sodium Selenite on the Histological Changes and Expression of Caspase-3 in the Testis of Monosodium Glutamate-Treated Rats: Light and Electron Microscopic Study

Nahla Reda Sarhan

Department of Histology and Cell Biology, Faculty of Medicine, Mansoura University, Mansoura, Egypt

Abstract

Monosodium glutamate (MSG) is a commonly used flavor enhancer that may contribute to male infertility. Sodium selenite is inorganic chemical form of selenium (Se). Se is best known as an antioxidant. This study was designed to investigate the possible ameliorating role of sodium selenite against MSG-induced testicular toxicity and histological changes. Forty male albino rats were allocated into four groups. Control group received distilled water, SE group received sodium selenite (0.25 mg/kg/day) dissolved in distilled water orally, MSG group received MSG (6 mg/g/day) dissolved in distilled water orally, and MSG + SE group received both MSG and sodium selenite for 45 days. Testicular samples were prepared for biochemical, light, and electron microscopic studies. Immunohistochemical staining for caspase-3 was done. MSG group demonstrated a significant increase in malondialdehyde level, marked damage of seminiferous tubules with a significant reduction in diameter and height of the lining epithelium. Spermatogenic cells showed disorganization, dark nuclei, reduction in number, and maturation arrest. Vacuolations of interstitial tissue and Leydig cells were also observed. Percent area of fibrosis and caspase-3 immunoexpression was significantly increased. Ultrastructurally, irregular tubular basement membrane and damaged germ cells were found. The spermatogenic, Sertoli, and Leydig cells showed irregular shrunken nuclei, cytoplasmic vacuolations, and swollen mitochondria. MSG + SE group showed much better histological and ultrastructural picture and improvement of the measured biochemical and morphometric parameters. Percent area of caspase-3 immunoexpression was significantly decreased. In conclusion, sodium selenite ameliorated the testicular damaging effect of MSG through reduction of oxidative stress and apoptosis.

Keywords: Caspase-3, monosodium glutamate, selenium, testis, ultrastructure

INTRODUCTION

Monosodium glutamate (MSG), the sodium salt of glutamic acid, consists of 78% of glutamic acid, 22% of sodium, and water. Glutamic acid is one of the most widespread amino acids that form the main component of most tissue proteins and is found in many natural protein-rich products.[1]

MSG is used as a flavor enhancer throughout the world.[2] It is commonly used as food additive in food industry, in restaurants and homes. It is present in many packaged foods.[3] However, abuse of MSG may occur due to its abundance mostly without appearing on the label in many food ingredients.[4] MSG stimulates the orosensory receptors and improving the palatability of meals; therefore, MSG has positive effects on appetite and leading to weight gain.[5]

Many previous studies were done studying the toxic effect of MSG in different animal's tissues. It was reported that high doses of MSG in animals damage the hypothalamic neurons and alter the neural control of reproductive hormone secretion through the hypothalamic–pituitary–adrenal axis.[6]

Address for correspondence: Dr. Nahla Reda Sarhan,
Department of Histology and Cell Biology, Faculty of Medicine,
Mansoura University, Mansoura, Egypt.
E-mail: nahlamohamedreda@yahoo.com, nahlaredasarhan@mans.edu.eg

Access this article online

Quick Response Code:

Website:
http://www.jmau.org/

DOI:
10.4103/JMAU.JMAU_2_18

Furthermore, MSG causes damage in the rat liver, kidney,[7,8] and cerebellum.[9] Furthermore, MSG has a toxic impact on the testis of rats which may be involved in male infertility.[10,11] Moreover, a significant oligozoospermia and abnormal sperm morphology were reported in male Wistar rats receiving MSG in a dose-dependent manner.[12]

Oxidative stress occurs when there is an imbalance between reactive oxygen species (ROS) production and its removal in cells.[13] MSG can induce oxidative damage in many organs by the generation of ROS, increased lipid peroxidation, and change in the activity of antioxidant enzymes.[14-16]

Selenium (Se) is an essential trace element important for human health.[17] Sodium selenite is the inorganic chemical form of Se.[18] High levels of Se found in cereals, fish, and meat.[19] Se is best known as an antioxidant that exerts its action through its incorporation into various selenoproteins, for example, glutathione peroxidases (GPxs) and thioredoxin reductases.[20,21] Se is essential for male reproduction and normal spermatogenesis; its deficiency affects the sperm number, motility, and fertility.[22,23] It was previously reported that Se has a protective effect against heavy metals induced testicular.[24] and cardiac toxicity[25] in experimental animals.

Caspase-3 is a member of cysteinyl aspartate-specific proteases that play a vital role in regulation of apoptosis.[26] Caspases are also essential for apoptotic death in the human seminiferous epithelium.[27] During spermatogenesis; a balance between cell survival and apoptosis is fundamentally required.[28]

Little information exists on the effect of Se on MSG-induced changes in the rat testicular tissue. Moreover, to our knowledge, no previous studies reveal this effect at the ultrastructural level. Hence, the present work was carried out to investigate the possible ameliorating effect of sodium selenite on the rat testicular structural, immunohistochemical, and ultrastructural changes that can be provoked by MSG treatment.

MATERIALS AND METHODS

Chemicals
MSG was obtained in the form of white crystalline powder from Sigma-Aldrich (France). Sodium Selenite (Apeldoorn, Holland) was obtained in the form of powder from Moustafa Salama for Chemicals and Medical Trading, Cairo, Egypt.

Animals and experimental protocol
A total of 40 adult male albino rats were used in this work. Their weights range from 180 to 200 g. The experimental protocol was approved by the Institutional Review Board of Mansoura Faculty of Medicine (R/17.02.110). The animals were maintained at separate cages in a controlled temperature of 22°C ± 2°C, with average humidity and under a 12 h light: 12 h dark schedule. Water and food were allowed *ad libitum*. All experimental procedures were carried out at Histology and Cell Biology department, Faculty of Medicine, Mansoura, Egypt. The rats were treated with the tested chemicals orally by the gastric tube for 45 days. They were randomly assigned into four groups (10 rats each). Control group received 1 ml of distilled water. SE group received sodium selenite (0.25 mg/kg/day) dissolved in distilled water.[29] MSG group received MSG (6 mg/g/day) dissolved in distilled water.[30] MSG + SE group received both MSG and sodium selenite (6 mg/g/day +0.25 mg/kg/day dissolved in distilled water) as the previous two groups

Obtaining the specimens
At the corresponding time of sacrifice, the animals were anesthetized intraperitoneally by pentobarbital (40 mg/kg). Then, intracardiac perfusion was done by 2.5% glutaraldehyde with 0.1 M phosphate buffer at pH 7.4 for partial fixation of the specimens. Both testicles were dissected out from the animals of all groups and processed for biochemical assay, light and electron microscopic studies.

Biochemical assay for malondialdehyde
Malondialdehyde (MDA) was determined in the testicular tissue as a biochemical marker for oxidative stress-induced lipid peroxidation. The tissue samples were homogenized in 5–10 ml cold buffer (50 mM potassium phosphate, pH 7.5) per gram tissue and centrifuged at 4000 rpm for 15 min at 4°C. The supernatant was collected and kept at −80°C to be used for colorimetric estimation of MDA according to thiobarbituric acid reaction described by Ohkawa *et al*.[31] using the kit provided by Bio-Diagnostics (Dokki, Giza, Egypt, Cat. No. MD 2529). The value is expressed as nmol/g tissue.

Light microscopic study
Samples from the right testis were fixed in 10% buffered neutral formalin and processed using the standard procedure to obtain paraffin blocks. Five micrometers thick serial sections were cut and stained with hematoxylin and eosin (H and E)[32] for the routine histological examination of the structural changes, Masson's trichrome stain[33] for collagen fibers' demonstration, and immunohistochemical stain with anti-caspase-3 antibody.

Immunohistochemical staining for caspase-3
Avidin-biotin-peroxidase technique[34] was used for the detection of activated caspase-3 as an apoptotic marker. Brown cytoplasmic or nuclear staining is considered positive reaction. After deparaffinization and rehydration of the sections, antigen retrieval was achieved by boiling sections in citrate buffer in a microwave. Endogenous peroxidase was blocked using H_2O_2. After blocking of nonspecific background with 10% serum-tris buffer for 20 min at room temperature, the sections were then incubated with the primary antibody anti-caspase-3 rabbit polyclonal antibody (catalog no RP096, Diagnostic Biosystems; USA,) diluted 1/100 at room temperature for 120 min. The slides were subsequently incubated with Biotinylated polyvalent secondary antibody and then incubated with avidin–biotin–peroxidase complex solution (LSAB 2 Kit; Dako). The reaction was visualized by adding 3,3′-diaminobenzidine tetrachloride to the sections. Hematoxylin was used to counterstain the sections. Slides stained with secondary antibody IgG only were used as

negative controls. Specimens from palatine tonsil were used as positive controls.

Electron microscopic study

Small specimens (1 mm³) from the left testis were fixed in 2.5% glutaraldehyde and 2% paraformaldehyde in a 0.1 M phosphate buffer (pH 7.4) overnight. Then, specimens were postfixed in 1% osmium tetroxide for 1 h at 4°C then washed three times in phosphate-buffered saline (10 min each). Semithin sections (1 μm) were cut using ultramicrotome (Leica ultracut UCT, Germany) and stained with 1% toluidine blue. Ultrathin sections (60–80 nm) were obtained and stained with uranyl acetate and lead citrate for 10 min each[35] to be examined by JEOL-JEM-100 SX transmission electron microscope in the Electron Microscopy unit, Faculty of Medicine, Tanta University, Egypt.

Morphometric study

Slides were photographed by a digital camera (Olympus; E420, China) installed on Olympus microscope with 0.5 × photo adaptor, using objective lens × 10 (TX31 Philippines). The images were then analyzed on Intel Core 13 based computer using VideoTesT Morphology software (VideoTesT, Russia, Saint-Petersburg) with a specific built-in procedure for calibrated distance and percent area % of fibrosis and immunoexpression. The diameter of transversely cut seminiferous tubules (STs), height of seminiferous epithelium (measured from the cells on the basement membrane till the most advanced cells toward the lumen), percent area % of blue stained collagenous fibers that indicate fibrosis, and percent area % of caspase-3 immunoexpression were quantified from ten nonoverlapping fields per rat, in each group from H and E, Masson's trichrome, and immuno-stained sections, respectively.

Statistical analysis

Statistical analysis for the data was done using Statistical Package for Social Science 17.0 (SPSS Inc., Chicago, USA). Comparisons between groups were carried out using analysis of variance followed by *post hoc* Tukey test. Data were represented as mean ± standard deviation. $P < 0.05$ was considered statistically significant.

RESULTS

Biochemical results

MDA level in the testicular tissue of MSG group was significantly higher ($P < 0.05$) than Control and SE groups. While it showed a significant reduction ($P < 0.05$) in MSG + SE group compared with MSG group, but it still significantly higher than Control and SE groups [Figure 1].

Light microscopic results

Hematoxylin and Eosin stain

The testis of Control and SE groups showed the normal histological appearance of the STs and the intervening interstitial tissue. Basement membrane was seen surrounding the tubules enclosing myoid cells. The tubules were lined with
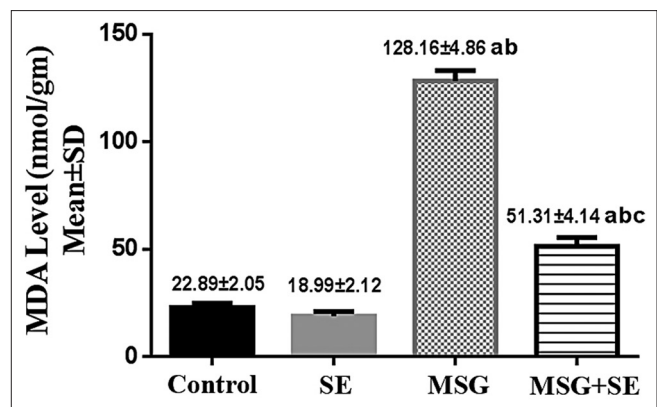

Figure 1: Changes in malondialdehyde level in the testicular tissue of different studied groups. Each bar represents mean ± standard deviation of ten animals in each group. Significance: *P* < 0.05. a: significance relative to Control group. b: significance relative to SE group. c: significance relative to MSG group

seminiferous epithelium that was formed of Sertoli cells and layers of spermatogenic cells that include spermatogonia, primary spermatocytes, spermatids, and spermatozoa. The spermatogonia with their dark nuclei were seen resting on the basement membrane. Primary spermatocytes were the largest cells in the spermatogenic series and showed nuclei with splitted chromatin. Near the lumen there were the spermatids; the early (rounded) and the late (elongated) ones. Many spermatozoa were seen in the tubular lumen. Leydig cells were found in the interstitial tissue between the tubules [Figure 2].

MSG group demonstrated remarkable histological changes. The STs were damaged, deformed, and irregular. There was a significant reduction ($P < 0.05$) in the mean diameter of the STs and mean height of their lining epithelium relative to Control and SE groups. The tubular basement membrane was irregular or interrupted. The spermatogenic cells showed disorganization, darkly stained nuclei, reduction in number, and maturation arrest up to early spermatid stage in some tubules. Few spermatozoa were also observed. Moreover, the cells showed detachment from the basement membrane, cytoplasmic vacuoles, empty areas, and vacuoles between them. Shrunken Sertoli cells with dark nuclei were also noticed. Widening of the intertubular space with congested blood vessels and reduction or hyalinization and vacuolations of the interstitial tissue was noticed. The Leydig cells were apparently reduced in number and showed vacuolations [Figures 3 and 4].

On the other hand, the histological changes in MSG + SE group were relatively ameliorated. The STs revealed a preserved morphology and were lined with all stages of spermatogenic cells and Sertoli cells. The diameter of the tubules and the height of seminiferous epithelium were significantly higher ($P < 0.05$) than MSG group with insignificant difference compared to Control and SE groups. However, some tubules showed some histological changes as a reduction in the number of spermatogenic cells with spacing and vacuolations between
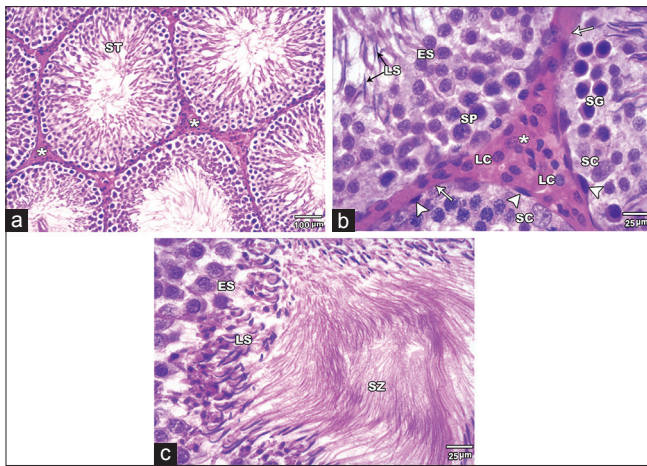
Figure 2: H and E stained sections of the Control group testis. (a and b): showing the seminiferous tubules (ST) and the interstitial tissue (asterisks) in between containing the Leydig cells (LC). Each tubule is surrounded by a basement membrane (arrows) and myoid cells (arrow heads) and lined with Sertoli cells (SC) and series of spermatogenic cells. They include spermatogonia (SG), primary spermatocytes (SP), early spermatids (ES) and late spermatids (LS). (C) showing the early spermatids (ES), late spermatids (LS) and many spermatozoa (SZ) filling the tubular lumen (A x100; B & C x 400)

them. The interstitial tissue and Leydig cells showed preserved structure [Figures 4 and 5].

Masson's trichrome stain

In control and SE groups, minimal amount of collagenous fibers was observed in the interstitial tissue between the tubules. However, MSG group demonstrated the excess amount of collagenous fibers in the interstitial tissue and around the blood vessels. MSG + SE group showed some collagenous fibers in the interstitial tissue and perivascular [Figure 6]. The mean percent area of fibrosis was significantly higher ($P < 0.05$) in MSG group relative to Control and SE groups. In contrast, it showed a significant reduction in MSG + SE group compared to MSG group but still higher than Control and SE groups [Figure 7].

Immunohistochemical staining for caspase-3

Negative to weak caspase-3 expression is found in the cytoplasm of the seminiferous epithelium and in the interstitial Leydig cells of the Control and SE groups. In MSG group, there was increased expression of caspase-3 in the cytoplasm and nuclei of the seminiferous epithelium. Leydig cells also showed strong caspase-3 expression. In MSG + SE, a weak-to-moderate caspase-3 expression was observed in the cytoplasm of the seminiferous epithelium and in Leydig cells [Figure 8]. The mean percent area of caspase-3 immunoexpression was significantly higher ($P < 0.05$) in MSG group compared to Control and SE groups. While it was significantly lower ($P < 0.05$) in MSG + Se group compared to MSG group but still higher than Control and SE groups [Figure 9].

Electron microscopic results

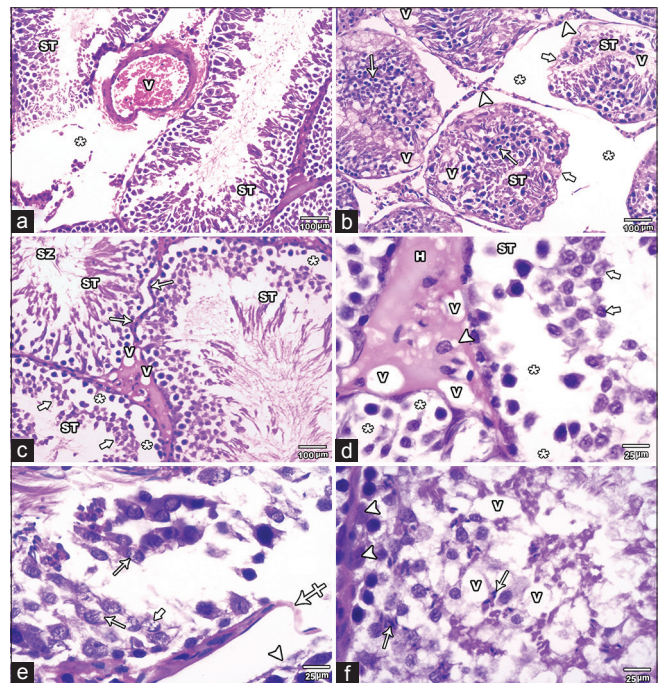In Control and SE groups, the STs were surrounded by thin

Figure 3: H and E stained testicular sections of MSG group.(a) showing degenerated STs with disorganized spermatogenic cells. Widening of the intertubular space (asterisks) with congested blood vessel (V) is also seen.(b) showing widening of the intertubular space (asterisks) with reduction in interstitial tissue (arrow heads). The seminiferous tubules (ST) appeared reduced in diameter, irregular (thick arrows) and deformed with few disorganized spermatogenic cells that have many darkly stained nuclei (arrows). Many vacuoles (V) are also seen among the spermatogenic cells. (c and d): showing distorted ST with irregularity of their basement membrane (arrows). The spermatogenic cells are apparently decreased in height and number up to the early spermatid stage (thick arrows) in some tubules. Empty areas (asterisks) are also found around and between the cells. Hyalinization (H) and vacuolations (V) of the interstitial tissue with decreased number and vacuolations (arrow head) of Leydig cells are noted. Few spermatozoa are seen in the lumen (SZ). (e) showing markedly degenerated tubules with detached spermatogenic cells (arrow head) from the basement membrane which appears interrupted at some areas (crossed arrow). The spermatogenic cells lost their normal arrangement and some show vacuolations (arrows). Karyolysis (thick arrow) is observed in some nuclei. (f) showing marked reduction in the number of the spermatogenic cells. Few late spermatids (arrows) are seen even in the basal part of the tubules. Vacuoles (V) among the cells and shrunken Sertoli cells with dark nuclei (arrow heads) are also noticed (A, B &C x100; D, E& F x400)

regular basement membrane enclosing myoid cells with flat central nuclei and lined with Sertoli cells and spermatogenic cells. The Sertoli cell lied on the basement membrane and showed a nucleus with a prominent nucleolus and the characteristic longitudinal fold. Its cytoplasm contained mitochondria, sER, and lipid droplets. The spermatogonia had a pale nucleus with a prominent nucleolus and showed peripheral clumps of chromatin. Mitochondria and rER were seen in the cytoplasm. The primary spermatocytes revealed large rounded nucleus and many mitochondria in their cytoplasm. Early spermatid was rounded with rounded
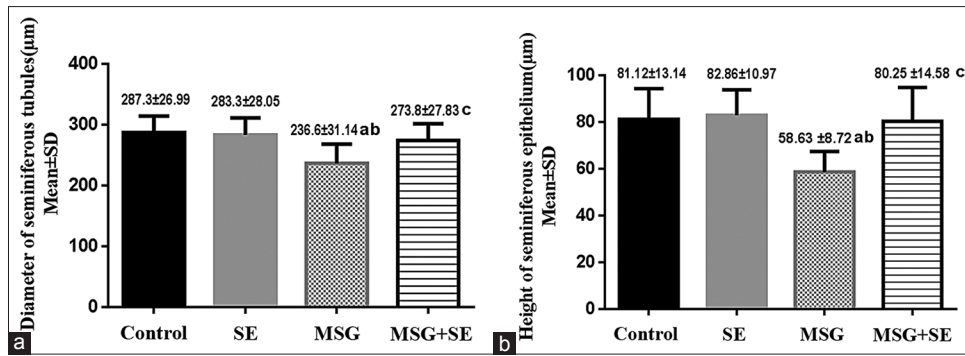
Figure 4: Changes in the diameter of seminiferous tubules (a) and height of their epithelium (b) in the different studied groups. Each bar represents mean ± standard deviation of ten animals in each group. Significance: *P* < 0.05. a: significance relative to control group. b: significance relative to SE group. c: significance relative to MSG group
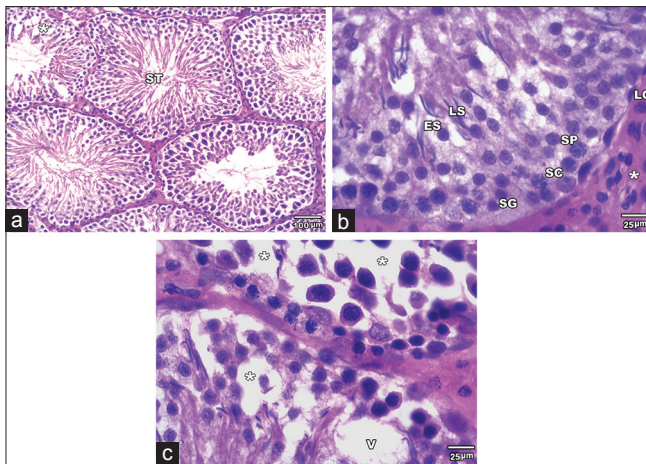

Figure 5: H and E stained sections of MSG+Se group testis. (a) showing seminiferous (ST) tubules with more or less intact histological structure. However; some damaged (asterisk) tubules are noticed. (b) The Seminiferous tubules are lined with more or less intact Sertoli cells (SC) and spermatogenic cells at all stages of differentiation (SG, SP, ES and LS). The interstitial tissue (asterisks) and Leydig cells (LC) have preserved morphology. (c) some tubules showing reduced number of spermatogenic cells with spacing (asterisks) and vacuolations (V) between them (A x100, B& C x400)

nucleus that covered on its proximal part by acrosomal cap and its vesicle. The cytoplasm showed peripherally situated vesicular mitochondria and Golgi complex. However, the late spermatid was elongated and formed of a head that surrounded by an acrosomal cap and contained a dark nucleus and a tail. The interstitial cell of Leydig demonstrated large euchromatic nucleus with peripherally arranged heterochromatin and prominent nucleolus. Many mitochondria, sER, and lipid droplets were noted in its cytoplasm [Figure 10].

MSG group displayed notable ultrastructural alterations. The STs were markedly damaged with irregularity and thickening of the basement membrane. The tubular lining cells were damaged and separated by wide intercellular spaces. Some cells showed shrunken or ruptured nuclei and large empty cytoplasmic areas. Sertoli cell exhibited irregular nucleus, swollen mitochondria,
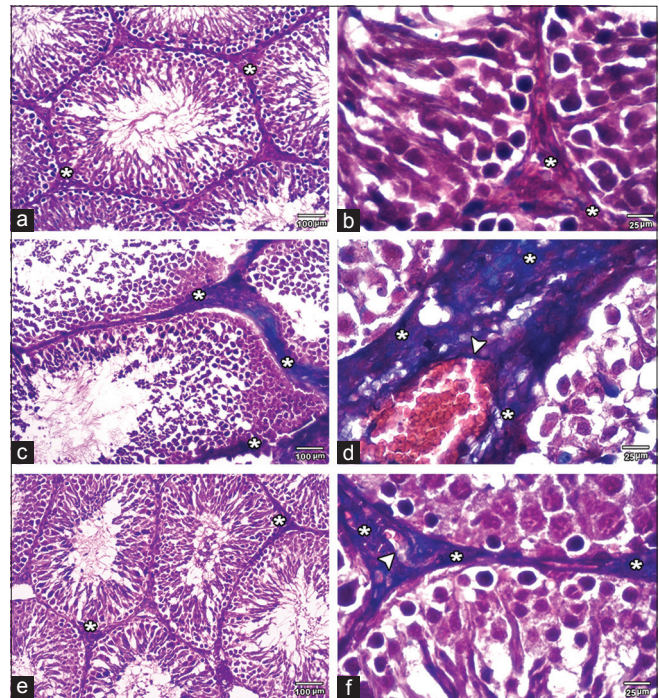

Figure 6: Masson's trichrome-stained sections of the testis among the different groups. (a and b) control group showing minimal amount of collagenous fibers in the interstitial tissue (asterisks) between the seminiferous tubules. (c and d) MSG group showing excessive amount of collagenous fibers in interstitial tissue (asterisks) and around (arrowhead) the blood vessels. (e and f) MSG + SE group showing some collagenous fibers in the interstitial tissue (asterisks) and around (arrowheads) blood vessels ([a, c, and e] ×100; [b, d, and f] ×400)

and numerous cytoplasmic vacuolations. Wide perinuclear space, swollen mitochondria, autophagic vacuoles, and vacuoles were observed in the spermatogonia. The primary spermatocytes appeared to have shrunken irregular nuclei with many clumps of heterochromatin. Their cytoplasm showed swollen mitochondria and many vacuoles. Early spermatids were malformed with the absence of acrosomal cap and showed large empty cytoplasmic areas. Late spermatids were abnormally found near the basal part of the STs. Moreover, the interstitial Leydig cell revealed irregular shrunken nucleus with
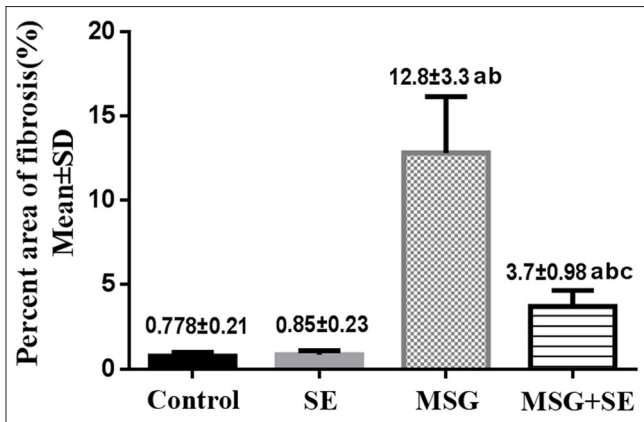
Figure 7: Changes in percent area of fibrosis in the different studied groups. Each bar represents mean ± standard deviation of ten animals in each group. Significance: *P* < 0.05. a: significance relative to control group. b: significance relative to SE group. c: significance relative to MSG group
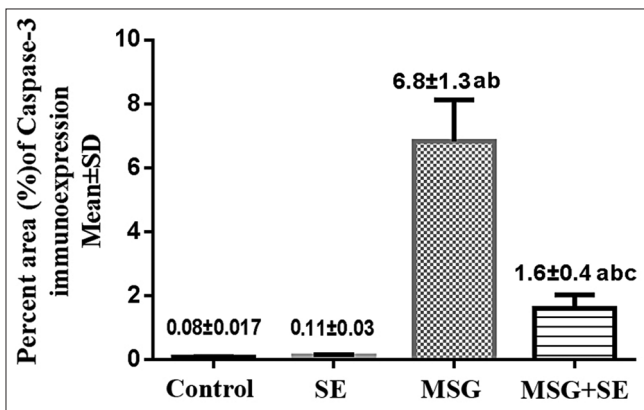

Figure 9: Changes in percent area of caspase-3 immunoexpression in the different studied groups. Each bar represents mean ± standard deviation of ten animals in each group. Significance: *P* < 0.05. a: significance relative to control group. b: significance relative to SE group. c: significance relative to MSG group

Figure 8: Caspase-3 expression in the testis of the studied group. (a and b) Control group revealed negative to weak caspase-3 expression in the cytoplasm of the seminiferous epithelium (arrows) and in interstitial cells of Leydig (arrowheads). (c and d) MSG group showing moderate-to-strong caspase-3 expression in the cytoplasm and nuclei of the seminiferous epithelium (arrows). Furthermore, the interstitial Leydig cells show strong caspase-3 expression (arrowheads). (e and f) MSG+SE group showing weak-to-moderate caspase-3 expression in the cytoplasm of the epithelium (arrows) and in the interstitial Leydig cells (arrowheads) (×400)

widening of the perinuclear space. Damaged mitochondria and vacuoles were also found the cytoplasm [Figure 11].

MSG + SE group demonstrated preserved testicular ultrastructure. The STs surrounded by thin regular basement membrane and were lined with intact Sertoli cells and other cells of spermatogenic series. However, there was some widening of the intercellular space. The interstitial tissue showed relatively intact Leydig cell contained some damaged mitochondria in the cytoplasm [Figure 12].

DISCUSSION

The current study revealed variable structural alterations in the testis of MSG group that provide evidences for the marked damage of the STs and degeneration of their lining cells and Leydig cells together with the observed maturation arrest that represented by decreased number of spermatogenic cells up to the early spermatid stage. These results coincide
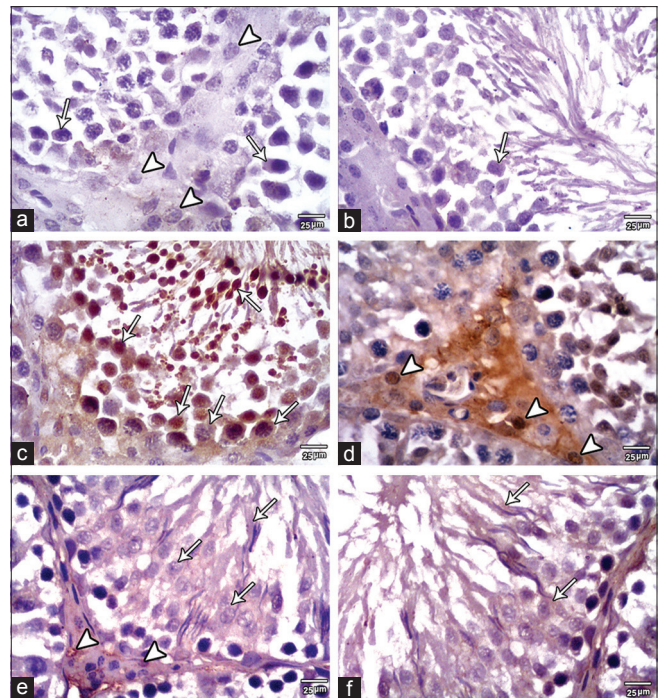
with the morphometric changes in the diameter of the STs and the height of their lining epithelium. Such findings were in consistent with previous studies on the effect of MSG in rat testis.[10,36] Kianifard[37] observed reduction in the diameter of STs and decreased number of primary spermatocytes and spermatids following MSG treatment in rats and mentioned that depopulation of germ cells led to tubular atrophy and indicated a reduction of cell divisions. The widening in the intertubular space that was observed in this study might be due to the atrophy and reduced tubular diameter. In contrast, Igwebuike *et al.*[38] and Okoye *et al.*[39] did not find any histological lesions in the testicular tissue of animals receiving MSG.

Rare studies were carried out to demonstrate the ultrastructural changes in the testis following exposure to MSG. The present study revealed many ultrastructural abnormalities in the spermatogenic cells, Sertoli cells, and Leydig cells of MSG group including cytoplasmic vacuolations, irregular shrunken nuclei with widening of perinuclear space, and swollen damaged mitochondria. Similar results were reported by Mohamed[40] in the MSG-treated adult rat testis. The cytoplasmic vacuolations observed in the cells might be damaged mitochondria or a sign of cellular toxicity and degeneration.
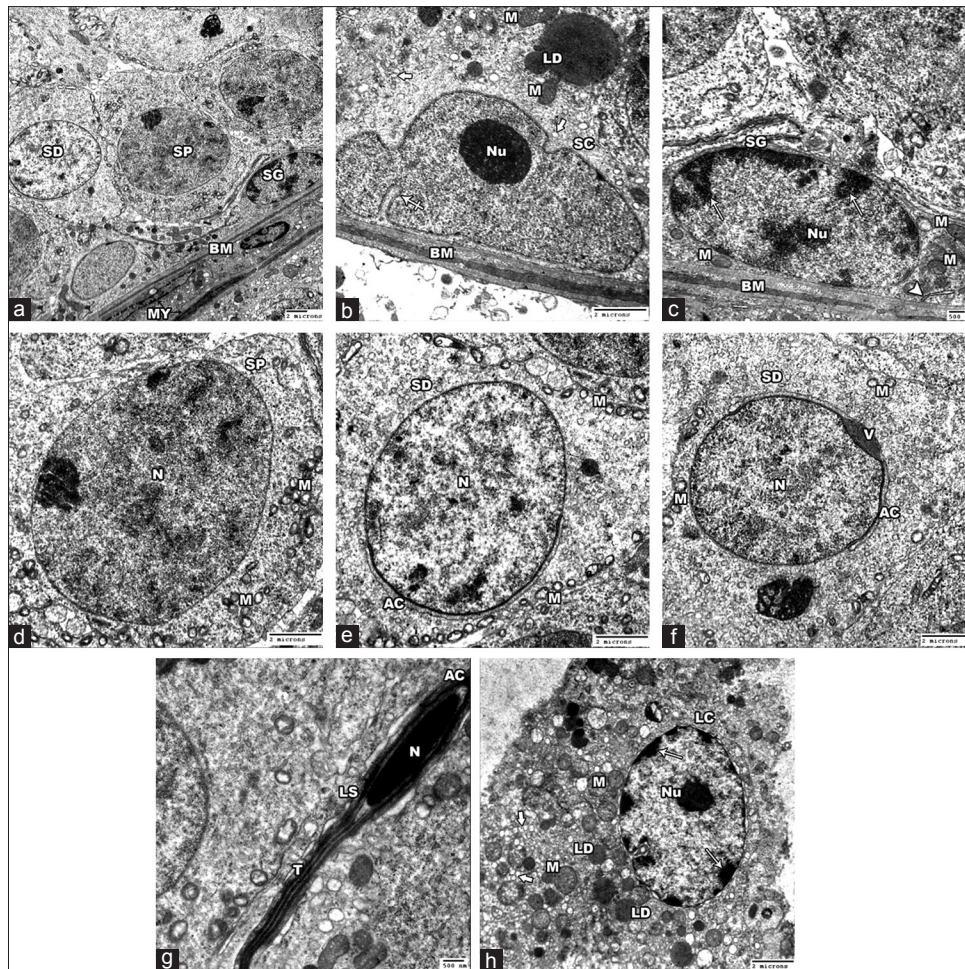
Figure 10: Electron micrographs of the Control group testis. (a) showing the spermatogonia (SG), primary spermatocyes (SP) and the spermatids (SD) lining a ST. Thin regular Basement membrane (BM) and Myoid cells (MY) are seen surrounding the tubules.(b) showing a Sertoli cell (SC) lying on BM. The nucleus has a characteristic longitudinal fold (crossed arrow) and a prominent nucleolus (Nu). Its cytoplasm contains mitochondria (M), lipid droplets (LD) and sER (thick arrows). (c-e): high magnification of A. (c) showing a regular BM and a spermatogonial cell (SG) that has a pale nucleus with prominent nucleolus (Nu) and peripheral chromatin clumps (arrows), mitochondria (M) and rER (arrow head). (d) the primary spermatocyte (SP) shows large rounded nucleus (N) and many mitochondria (M) in the cytoplasm. (e and f) showing early spermatids (SD) with rounded nuclei (N) that are covered on the proximal part by the acrosomal cap (AC) and its vesicle (V). Peripherally arranged vesicular mitochondria (M) are found in the cytoplasm. (g) showing late spermatid (LS) formed of head that contains nucleus (N) and surrounded by acrosomal cap (AC) and a tail (T). (h) the Leydig cell (LC) revealed large euchromatic nucleus with peripheral heterochromatin (arrows) and prominent nucleolus (Nu). The cytoplasm shows many mitochondria (M), lipid droplets (LD) and sER (thick arrow) (Ax 1000; C x 3000 B, D, E &F x 2500; G x 4000; H x 2000)

The toxic effect of MSG and all the testicular changes and maturation arrest that were observed in the current study in the testis of MSG group could be explained by different mechanisms. One of these mechanisms is the direct effect of MSG on the glutamate receptors and transporters that are expressed in the epithelial cells of STs.[41,42] Another mechanism is the indirect effect of MSG on testis. MSG is neurotoxic, when found in high concentration it causes excessive glutamate receptor activation and can induce neuronal death.[43] Hypothalamic neuronal cell death[44] and reduction in the level of luteinizing hormone (LH), FSH, and testosterone and decreased sperm count[36-38] were previously reported after administration of MSG in mice and rats. Hence, the damage of hypothalamic neurons by MSG may cause disruption of the hypothalamic–pituitary–gonadal axis that control the normal

spermatogenesis and testosterone secretion by the Leydig cells[45] and can lead to structural and functional alterations of testicular tissue.

Oxidative damage is considered one of the most important mechanisms involved in MSG-induced testicular toxicity. MDA is one of the major products of oxidative stress-induced lipid peroxidation and its level is an indicator for the degree of lipid peroxidation.[46] In the current study, the observed significant increase in MDA level in testicular tissue of MSG group when compared to the Control group indicating the development of oxidative stress. It was previously reported that MSG generates ROS that causes an increase in lipid peroxidation. In addition, MSG decreases the endogenous-free radical scavengers such as antioxidant enzymes, glutathione, and ascorbic acid that protect and stabilize the biomembranes
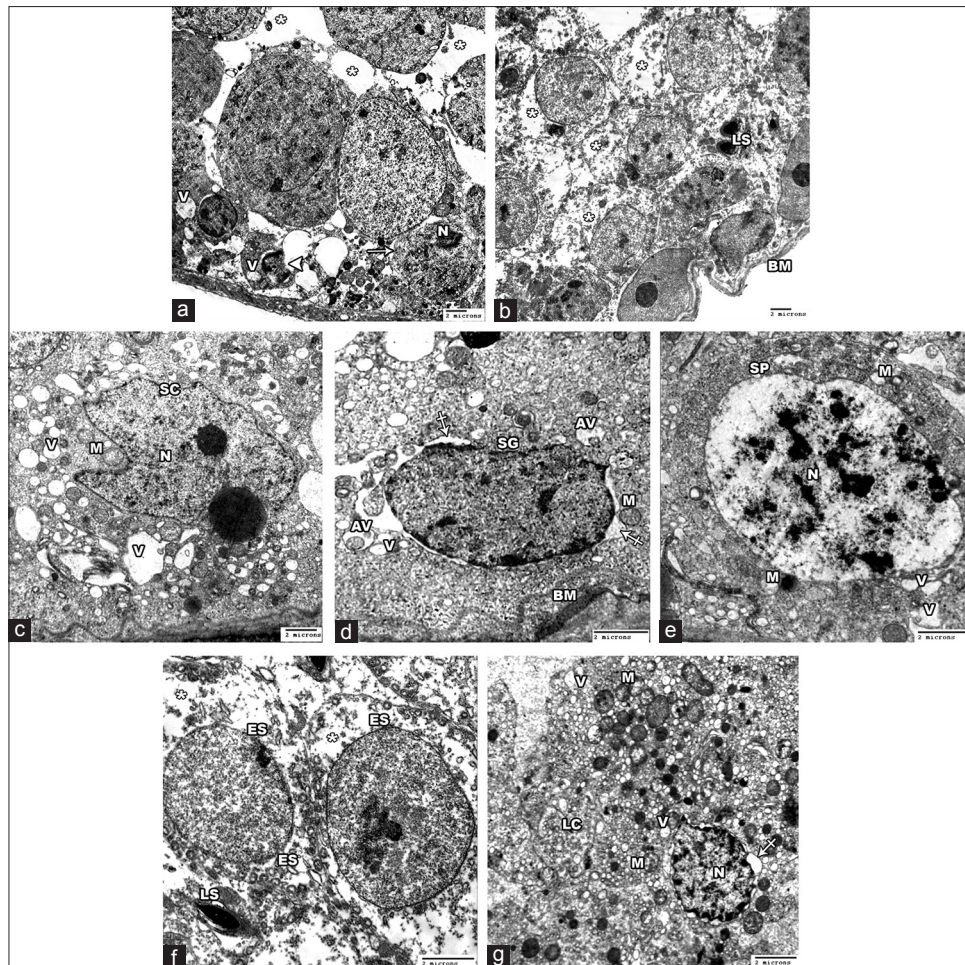
Figure 11: Electron micrographs of the testis of MSG group. (a) showing a damaged tubule with wide intercellular spaces (asterisks). Some spermatogenic cells (arrow) show shrunken nuclei (N). Others shows ruptured nucleus (arrow heads) and cytoplasmic vacuolations (V). (b) A markdly damaged tubule with irregular basement membrane (BM) is shown. The cytoplasm of spermatogenic cells revealed large empty areas (asterisks). Note late spermatids (LS) are abnormally placed near the basal part of tubule. (c) showing a Sertoli cell (SC) with irregular nucleus (N) , swollen mitochondria (M) and multiple cytoplasmic vacuoles (V) of variable size. (d) showing a thick irregular basement membrane (BM) and a spermatogonial cell (SG) with wide perinuclear space (crossed arrows), swollen mitochondria (M), autophagic vacuoles (AV) and vacuoles (V). (e) A primary spermatocyte (SP) revealed large nucleus (N) with heterochromatin clumps, swollen mitochondria (M) and vacuoles (V). (f) showing two malformed ealy spermatids (ES) with absence of acrosomal cap. Large empty cytoplasmic areas (asterisks) are observed. A late spermatid (LS) is seen (g) showing a Leydig cell (LC) with irregular shrunken nucleus (N) with more heterochromatin and wide perinuclear space (crossed arrow). Damaged mitochondria (M) and vacuoles (V) is noted in the cytoplasm (A&B x 1000; C x 1500; D, E & F x 2500; G x 2000)

from the lipid peroxidation and oxidative damage.[14,16,47] Nayanatara *et al*.[47] stated that decreased level of ascorbic acid by MSG in the testis leads to uncontrolled oxidative damage that destroys most of the germ cells and affects the spermatogenesis. Excessive free radicals can lead to oxidative DNA damage and cellular death. Mitochondria are the main source of ROS and are particularly susceptible to oxidative stress that leading to mitochondrial DNA damage, mitochondrial dysfunction, change in permeability, and structure.[48] This might explain the mitochondrial swelling and damage observed in the spermatogenic cells, Sertoli, and Leydig cells in the present study.

Excess collagenous fibers were observed in the intertubular interstitial tissue and perivascular in Masson's trichrome-stained sections of MSG group. Furthermore, the percent area of

fibrosis was significantly higher as compared to control group. Similarly, MSG causes renal interstitial fibrosis in rats.[49] The oxidative stress secondary to MSG may contribute to the observed testicular fibrosis. It has been documented that ROS can induce the transformation of fibroblasts to the more synthetic myofibroblasts.[50]

Apoptosis is a physiological process that controls cell number in the testicular tissue and removes the defective germ cells during spermatogenesis. However, excessive apoptosis causes destruction of male reproductive function.[51] In the present study, MSG group showed strong caspase-3 expression in the cytoplasm and nuclei of tubular cells and Leydig cells and a significant increase in the percent area of caspase-3 immunoexpression relative to the control indicating that MSG elicits apoptosis in the rat testis. These findings were in harmony
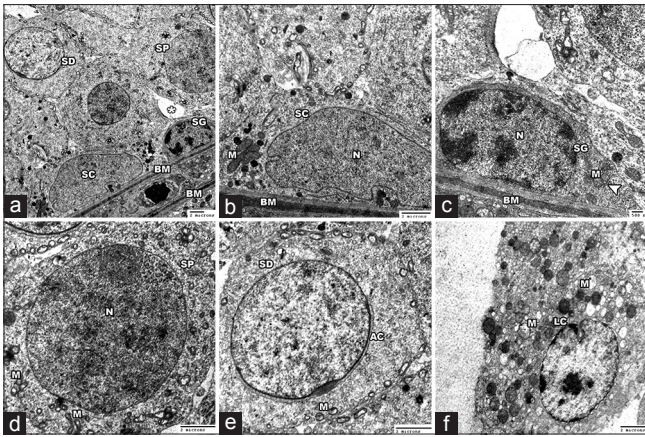
Figure 12: Electron micrographs of the testis of MSG+Se group. (a) revealed a preserved seminiferous tubule with thin regular basment membrane (BM). The Sertoli cell (SC), spermatogonia (SG) , primary spermatocytes (SP) and the spermatids (SD) show a relative intact fine structure. Some widening of the intercellular space is found (asterisks). (b-e) High magnification of A showing intact ultrastucture of BM and the tubular lining cells. Sertoli cell (SC) with its characteristic nucleus (N) showed healthy mitochondria (M). spermatogonial cell (SG) showed intact nucleus (N), mitochondria (M), rER (arrow head). Primary spermatocyte (SP) with large rounded nucleus (N) and intact mitochondria (M) is seen. The spermatid (SD) with acrosomal cap (AC) showed mitochondria (M) in the cytoplasm. (f) showing intact Leydig cell (LC), however some damaged mitochondria (M) are seen in the cytoplasm (A x 1000; B x 2000; C x 3000; D&E x 2500; F x 2000)

with Abd-Ella *et al.*,[11] who observed increase in caspase-3 expression in the liver and testis of MSG-treated rats. Caspase-3 is a key mediator of apoptosis. Two main apoptotic pathways were reported extrinsic (receptor pathway) and intrinsic (mitochondrial pathway). Both pathways lead to activation of effector caspase-3 that cleaves intracellular substrates, resulting in dramatic morphological and biochemical changes of apoptosis.[52] Although the cytoplasmic localization of procaspase-3, it was reported that active caspase-3 translocated from the cytoplasm to the nucleus after induction of apoptosis leading to the nuclear morphological changes (e.g. chromatin condensation) of the apoptotic cells.[53] This might explain the noticed caspase-3 expression in the nuclei of the testicular cells and the darkly stained, irregular shrunken nuclei observed in this study in MSG group. ROS and the resulting oxidative stress can cause cell death by triggering the two apoptotic pathways.[54] Hence, in the current study, the increased expression of caspase-3 in MSG group might be caused by the induced oxidative stress by MSG.

In the present work, MSG + SE group showed marked improvement of the structural ultrastructural, biochemical, and morphometric alterations of the testicular tissue. Significant reduction of MDA level, percent area of fibrosis, and caspase-3 expression was observed as compared to MSG group. Such improvement clearly indicates protective mechanisms of Se which could be explained by its antioxidant action. These results were in consistent with previous studies. Hamza and Al-Harbi[30] reported that Se decreases lipid peroxidation, increases the

activity of catalase, superoxide dismutase and GPx, and reduces the histopathological changes induced by MSG in rats. Se also decreases the oxidative damage caused by other toxic agents in the testicular tissue of rats.[55] It has been shown that Se could protect against hepatic fibrosis by attenuating the oxidative damage and decrease expression of collagen and alpha-smooth muscle actin.[56] Kaur and Bansal[57] observed that Se protects against heat-induced apoptosis in the testis through modulation of oxidative stress. It decreases the production of ROS, reduces apoptotic index of spermatogenic cells, and expression of apoptotic factors, for example, caspase-3 and 9. Se also can protect against radiation-induced apoptosis.[58]

Se is an important constituent of the antioxidant system through its integration into many selenoproteins and enzymes. GPxs are a large family of antioxidant selenoenzymes that reduce hydrogen peroxides and lipids peroxides into water, thus preserving membranes integrity, reduces oxidative damage of lipids and DNA.[59] GPx 4 is found in high concentration in testis and protects the developing sperm cells against oxidative DNA damage.[60,61]

Other possible explanation for the improvement of the testicular changes in MSG + SE group is through the effect of Se on testosterone and LH secretion. It has been mentioned that Se administration increases the level of testosterone and LH hormones.[55] Behne *et al.*[62] observed decreased serum testosterone and reduced diameter of ST in Se-deficient rats. They stated that Se is important for synthesis of testosterone and normal spermatogenesis and its deficiency can indirectly affect the testicular morphology.

Conclusion

Long-term consumption of MSG can induce biochemical, structural, and ultrastructural alterations in the rat testicular tissue through induction of oxidative stress which may affect male fertility. Moreover, supplementation of Se is beneficial in ameliorating the testicular damaging effects of MSG by reducing the oxidative damage and apoptosis through decreased expression of caspase-3.

Financial support and sponsorship
Nil.

Conflicts of interest
There are no conflicts of interest.

References

1. Samuels A. The toxicity/safety of processed free glutamic acid (MSG): A study in suppression of information. Account Res 1999;6:259-310.
2. Atasevan N, Yüzbaşıoğlu D, Keskin AÇ, Ünal F. Genotoxicity of monosodium glutamate. Food Chem Toxicol 2016;91:8-18.
3. Bojanić V, Bojanić Z, Najman S, Savić T, Jakovljević V, Najman S, *et al.* Diltiazem prevention of toxic effects of monosodium glutamate on ovaries in rats. Gen Physiol Biophys 2009;28:149-54.
4. Egbuonu AC, Obidoa O, Ezeokonkwo CA, Ezeanyika LU, Ejikeme PM. Hepatotoxic effects of low dose oral administration of monosodium glutamate in male albino rats. Afr J Biotechnol 2009;8:3031-5.
5. Rogers PJ, Blundell JE. Umami and appetite: Effects of monosodium

glutamate on hunger and food intake in human subjects. Physiol Behav 1990;48:801-4.

6. Seo HJ, Ham HD, Jin HY, Lee WH, Hwang HS, Park SA, *et al.* Chronic administration of monosodium glutamate under chronic variable stress impaired hypothalamic-pituitary-adrenal axis function in rats. Korean J Physiol Pharmacol 2010;14:213-21.

7. Ortiz GG, Bitzer-Quintero OK, Zárate CB, Rodríguez-Reynoso S, Larios-Arceo F, Velázquez-Brizuela IE, *et al.* Monosodium glutamate-induced damage in liver and kidney: A morphological and biochemical approach. Biomed Pharmacother 2006;60:86-91.

8. El-Meghawry El-Kenawy A, Osman HE, Daghestani MH. The effect of Vitamin C administration on monosodium glutamate induced liver injury. An experimental study. Exp Toxicol Pathol 2013; 65:513-21.

9. Hashem HE, El-Din Safwat MD, Algaidi S. The effect of monosodium glutamate on the cerebellar cortex of male albino rats and the protective role of Vitamin C (histological and immunohistochemical study). J Mol Histol 2012;43:179-86.

10. Alalwani AD. Monosodium glutamate induced testicular lesions in rats (histological study). Middle East Fertil Soc J 2013;19:274-80.

11. Abd-Ella EM, Mohamed A, Mohamed A. Attenuation of monosodium glutamate-induced hepatic and testicular toxicity in albino rats by *Annona muricata* Linn. (*Annonaceae*) leaf extract. J Pharm Biol Sci 2016;11:61-9.

12. Onakewhor J, Oforofuo I, Singh S. Chronic administration of monosodium glutamate induces oligozoospermia and glycogen accumulation in Wistar rat testes. Afr J Reprod Health 1998;2:190-7.

13. Bashan N, Kovsan J, Kachko I, Ovadia H, Rudich A. Positive and negative regulation of insulin signaling by reactive oxygen and nitrogen species. Physiol Rev 2009;89:27-71.

14. Onyema OO, Farombi EO, Emerole GO, Ukoha AI, Onyeze GO. Effect of Vitamin E on monosodium glutamate induced hepatotoxicity and oxidative stress in rats. Indian J Biochem Biophys 2006;43:20-4.

15. Paul MV, Abhilash M, Varghese MV, Alex M, Nair RH. Protective effects of α-tocopherol against oxidative stress related to nephrotoxicity by monosodium glutamate in rats. Toxicol Mech Methods 2012;22:625-30.

16. Farombi EO, Onyema OO. Monosodium glutamate-induced oxidative damage and genotoxicity in the rat: Modulatory role of Vitamin C, Vitamin E and quercetin. Hum Exp Toxicol 2006;25:251-9.

17. Mistry HD, Broughton Pipkin F, Redman CW, Poston L. Selenium in reproductive health. Am J Obstet Gynecol 2012;206:21-30.

18. Puspitasari IM, Abdulah R, Yamazaki C, Kameo S, Nakano T, Koyama H, *et al.* Updates on clinical studies of selenium supplementation in radiotherapy. Radiat Oncol 2014;9:125.

19. Tinggi U, Reilly C, Patterson CM. Determination of selenium in foodstuffs using spectrofluorometry and hydride generation atomic absorption spectrometry. J Food Compost Anal 1992;5:269-80.

20. Kryukov GV, Castellano S, Novoselov SV, Lobanov AV, Zehtab O, Guigó R, *et al.* Characterization of mammalian selenoproteomes. Science 2003;300:1439-43.

21. Fritz H, Kennedy D, Fergusson D, Fernandes R, Cooley K, Seely A, *et al.* Selenium and lung cancer: A systematic review and meta analysis. PLoS One 2011;6:e26259.

22. Shalini S, Bansal MP. Role of selenium in regulation of spermatogenesis: Involvement of activator protein 1. Biofactors 2005;23:151-62.

23. Flohé L. Selenium in mammalian spermiogenesis. Biol Chem 2007;388:987-95.

24. Saïd L, Banni M, Kerkeni A, Saïd K, Messaoudi I. Influence of combined treatment with zinc and selenium on cadmium induced testicular pathophysiology in rat. Food Chem Toxicol 2010;48:2759-65.

25. Bhattacharjee S, Pal S. Additive protective effects of selenium and Vitamin E against arsenic induced lipidemic and cardiotoxic effects in mice. Int J Pharm Pharm Sci 2014;6:406-13.

26. Fischer U, Schulze-Osthoff K. Apoptosis-based therapies and drug targets. Cell Death Differ 2005;12 Suppl 1:942-61.

27. Li H, Xu L, Dunbar JC, Dhabuwala CB. Role of mitochondrial cytochrome c in cocaine-induced apoptosis in rat testes. Urology 2003;61:646-50.

28. Dasari VR, Veeravalli KK, Saving KL, Gujrati M, Fassett D, Klopfenstein JD, *et al.* Neuroprotection by cord blood stem cells against glutamate-induced apoptosis is mediated by Akt pathway. Neurobiol Dis 2008;32:486-98.

29. Koyuturk M, Yanardag R, Bolkent S, Tunali S. The potential role of combined anti-oxidants against cadmium toxicity on liver of rats. Toxicol Ind Health 2007;23:393-401.

30. Hamza RZ, Al-Harbi MS. Monosodium glutamate induced testicular toxicity and the possible ameliorative role of Vitamin E or selenium in male rats. Toxicol Rep 2014;1:1037-45.

31. Ohkawa H, Ohishi N, Yagi K. Assay for lipid peroxides in animal tissues by thiobarbituric acid reaction. Anal Biochem 1979;95:351-8.

32. Gamble M, Wilson L. The hematoxylin and eosin. In: Bancroft JD, Gamble M, editors. Theory and Practice of Histological Techniques. 5th ed. London, New York, Edinburgh, Philadelphia: Churchill Livingstone; 2002. p. 130.

33. Jones ML, Bancroft JD, Gamble M. Connective tissue and stains. In: Bancroft JD, editor. Theory and Practice of Histological Techniques. 6th ed. New York: Elsevier Health Sciences, Churchill Livingstone; 2008. p. 150.

34. Gu X, Herrera GA. Expression of eNOS in kidneys from hypertensive patients. Int J Nephrol Renovasc Dis 2010;3:11-9.

35. Woods AE, Stirling JW. Electron microscopy. In: Bancroft JD, Gamble M, editors. Theory and Practice of Histological Techniques. 6th ed. London, New York: Churchill Livingstone; 2008. p. 601-36.

36. Sakr SA, Badawy GM. Protective effect of curcumin on monosodium glutamate-induced reproductive toxicity in male albino rats. Glob J Pharmacol 2013;7:416-22.

37. Kianifard D. Microscpic study of testicular tissue structure and spermatogenesis following term dose dependent administration of monosodium glutamate in adult diabetic rats. Rom J Diabetes Nutr Metab Dis 2016;23:147-58.

38. Igwebuike UM, Ochiogu IS, Ihedinihu BC, Ikokide JE, Idika IK. The effects of oral administration of monosodium glutamate (msg) on the testicular morphology and cauda eipididymal sperm reserves of young and adult male rats. Vet Archiv 2011;81:525-34.

39. Okoye CN, Ochiogu IS, Onah CE. The effects of monosodium l-glutamate administration on the reproduction and serum biochemistry of adult male rabbits. Vet Med 2016;61:141-7.

40. Mohamed IK. The effect of oral dosage of monosodium glutamate applied for short-and long-terms on the histology and ultrastructure of testes of the adult rats. J Anim Vet Adv 2012;11:124-33.

41. Gill SS, Mueller RW, McGuire PF, Pulido OM. Potential target sites in peripheral tissues for excitatory neurotransmission and excitotoxicity. Toxicol Pathol 2000;28:277-84.

42. Takarada T, Hinoi E, Balcar VJ, Taniura H, Yoneda Y. Possible expression of functional glutamate transporters in the rat testis. J Endocrinol 2004;181:233-44.

43. Mattson MP. Glutamate and neurotrophic factors in neuronal plasticity and disease. Ann N Y Acad Sci 2008;1144:97-112.

44. Park CH, Choi SH, Piao Y, Kim S, Lee YJ, Kim HS, *et al.* Glutamate and aspartate impair memory retention and damage hypothalamic neurons in adult mice. Toxicol Lett 2000;115:117-25.

45. McLachlan RI, Wreford NG, O'Donnell L, de Kretser DM, Robertson DM. The endocrine regulation of spermatogenesis: Independent roles for testosterone and FSH. J Endocrinol 1996;148:1-9.

46. Karaboduk H, Uzunhisarcikli M, Kalender Y. Protective effects of sodium selenite and Vitamin E on mercuric chloride-induced cardiotoxicity in male rats. Braz Arch Biol Technol 2015;58:229-38.

47. Nayanatara AK, Vinodini NA, Damodar G, Ahemed B, Ramaswamy CR, Shabarinath M, *et al.* Role of ascorbic acid in monosodium glutamate mediated effect on testicular weight, sperm morphology and sperm count, in rat testis. J Chin Clin Med 2008;3:1-5.

48. Guo C, Sun L, Chen X, Zhang D. Oxidative stress, mitochondrial damage and neurodegenerative diseases. Neural Regen Res 2013;8:2003-14.

49. Sharma A, Prasongwattana V, Cha'on U, Selmi C, Hipkaeo W, Boonnate P, *et al.* Monosodium glutamate (MSG) consumption is associated with urolithiasis and urinary tract obstruction in rats. PLoS One 2013;8:e75546.

50. Sampson N, Koziel R, Zenzmaier C, Bubendorf L, Plas E, Jansen-Dürr P, *et al.* ROS signaling by NOX4 drives

fibroblast-to-myofibroblast differentiation in the diseased prostatic stroma. Mol Endocrinol 2011;25:503-15.

51. Print CG, Loveland KL. Germ cell suicide: New insights into apoptosis during spermatogenesis. Bioessays 2000;22:423-30.

52. Elmore S. Apoptosis: A review of programmed cell death. Toxicol Pathol 2007;35:495-516.

53. Kamada S, Kikkawa U, Tsujimoto Y, Hunter T. Nuclear translocation of caspase-3 is dependent on its proteolytic activation and recognition of a substrate-like protein(s). J Biol Chem 2005;280:857-60.

54. Ryter SW, Kim HP, Hoetzel A, Park JW, Nakahira K, Wang X, *et al.* Mechanisms of cell death in oxidative stress. Antioxid Redox Signal 2007;9:49-89.

55. Sakr SA, Mahran HA, Nofal AE. Effect of selenium on carbimazole-induced testicular damage and oxidative stress in albino rats. J Trace Elem Med Biol 2011;25:59-66.

56. Liu Y, Liu Q, Ye G, Khan A, Liu J, Gan F, *et al.* Protective effects of selenium-enriched probiotics on carbon tetrachloride-induced liver fibrosis in rats. J Agric Food Chem 2015;63:242-9.

57. Kaur S, Bansal MP. Protective role of dietary-supplemented selenium and Vitamin E in heat-induced apoptosis and oxidative stress in mice testes. Andrologia 2015;47:1109-19.

58. Puspitasari IM, Yamazaki C, Abdulah R, Putri M, Kameo S, Nakano T, *et al.* Protective effects of sodium selenite supplementation against irradiation-induced damage in non-cancerous human esophageal cells. Oncol Lett 2017;13:449-54.

59. Brigelius-Flohé R, Banning A, Schnurr K. Selenium-dependent enzymes in endothelial cell function. Antioxid Redox Signal 2003;5:205-15.

60. Beckett GJ, Arthur JR. Selenium and endocrine systems. J Endocrinol 2005;184:455-65.

61. Safarinejad MR, Safarinejad S. Efficacy of selenium and/or N-acetyl-cysteine for improving semen parameters in infertile men: A double-blind, placebo controlled, randomized study. J Urol 2009;181:741-51.

62. Behne D, Weiler H, Kyriakopoulos A. Effects of selenium deficiency on testicular morphology and function in rats. J Reprod Fertil 1996;106:291-7.